Inferring Urban Land Use from Satellite Sensor Images Using Kernel-Based Spatial Reclassification

M.J. Barnsley and S.L. Barr

Abstract

Per-pixel classification algorithms are poorly equipped to monitor urban land use *in images acquired by the current generation of high spatial resolution satellite sensors. This is because urban areas commonly comprise a complex spatial assemblage of spectrally distinct* land-cover *types. In this study, a technique is described that attempts to derive information on urban land use in two stages. The first involves classification of the image into broad land-cover types. In the second stage, referred to as spatial reclassification, the classified pixels are grouped into discrete land-use categories on the basis of* both *the frequency* and *the spatial arrangement of the land-cover labels within a square kernel. The application of this technique, known as* SPARK *(*SPAtial Reclassification Kernel*), is demonstrated using a* SPOT-1 HRV *multispectral image of southeast London, England. Preliminary results indicate that* SPARK *can be used to distinguish quite subtle differences of land use in urban areas.*

Introduction

While satellite sensor technology has been used with some success to monitor land use in images of agricultural areas, much less satisfactory results are generally reported for urban scenes (Forster, 1985; Toll, 1985; Barnsley *et al.*, 1989; Sadler and Barnsley, 1990). Initially, this disparity was attributed to the relatively coarse spatial resolution of early Earth-resources sensors, such as the Landsat Multispectral Scanning System (MSS) (Jackson *et al.*, 1980; Forster, 1980). By averaging the spectral response of buildings, roads, trees, grass and other component elements of urban scenes within their large instantaneous field-of-view (IFOV), these sensors tended to produce broad, composite signals for urban areas. Consequently, it was often difficult to distinguish between different categories of urban land use in the resultant images. Moreover, the "blocky" appearance of these images inhibited accurate delineation of the urban-rural boundary.

Unfortunately, the use of higher resolution data from the current generation of satellite sensors has not always yielded the improvements anticipated (Toll, 1985; Forster, 1985; Martin *et al.*, 1988). Indeed, some studies report a reduction in the accuracy with which different urban land uses can be distinguished in such images, relative to that obtained using coarser resolution data (Haack *et al.*, 1987; Martin *et al.*, 1988). This apparently paradoxical phenomenon has been ascribed to the problem of "scene noise" (Gastellu-Etchegorry, 1990; Gong and Howarth, 1990). In other words, as the spatial resolution of the sensor increases, individual scene elements (e.g., buildings, roads, and open spaces) begin to dominate the detected response of each pixel; therefore, the spectral response of urban areas as a whole becomes more varied, making consistent classification of land use problematic (Gastellu-Etchegorry, 1990).

Although it is tempting to set this problem in the context of inadequate or inappropriate sensor spatial resolution, it is perhaps more accurately expressed in terms of the limitations of commonly used information extraction techniques; in particular, standard, per-pixel, multispectral classification algorithms. The fundamental problem involved in producing accurate land-use maps of towns and cities from remotely sensed images is that urban areas comprise a complex spatial assemblage of land-cover types, each of which may have different spectral reflectance characteristics (Wharton, 1982a; Wharton, 1982b; Gong and Howarth, 1990; Barnsley *et al.*, 1991; Eyton, 1993). Unfortunately, per-pixel classification algorithms are poorly equipped to deal with this type of spatial variability, because they assign each pixel to one of the candidate classes solely on the basis of its spectral reflectance properties (Woodcock and Strahler, 1987; Barnsley *et al.*, 1991; Barnsley and Barr, 1992). The location of the pixel within the image and the relationship between its spectral response and that of its neighbors are not taken into account. A further problem for supervised, per-pixel classification is that it is extremely difficult to define suitable training sets for many categories of urban land use, due to the variation in the spectral response of their component land-cover types (Forster, 1985; Gong and Howarth, 1990; Barnsley *et al.*, 1991). Thus, the training statistics may exhibit both a multimodal distribution and a large standard deviation in each spectral waveband (Sadler *et al.*, 1991). The implication of the former is that the training statistics for urban areas violate one of the basic assumptions of the widely used maximum-likelihood decision rule, namely, that the pixel values follow a multivariate normal distribution. The effect of the latter is often to produce a pronounced overlap between urban and non-urban land-use categories in the multispectral

Remote Sensing Unit, Department of Geography, University College London, 16, Bedford Way, London WC1H 0AP, United Kingdom.

M.J. Barnsley is presently with the Department of Geography, University of Wales Swansea, Singleton Park, Swansea SA2 8PP, United Kingdom.

S.L. Barr is presently with the Department of Geography, University of Manchester, Mansfield Cooper Building, Oxford Road, Manchester M13 9PL, United Kingdom.

Photogrammetric Engineering & Remote Sensing, Vol. 62, No. 8, August 1996, pp. 949–958.

0099-1112/96/6208–949$3.00/0

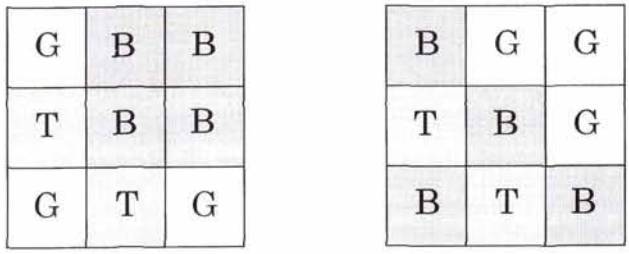

a) Commercial / Industrial b) Residential

Key: B = Building; T = Tree; G = Grass.

Figure 1. Simulated 3- by 3-pixel windows showing the possible distributions of land cover types for two urban land-use categories.

feature space. This may be further compounded by the fact that the *mean* spectral response for the urban classes will differ from those of the non-urban classes in a somewhat arbitrary and unpredictable manner, depending on the location of the training areas (Barnsley *et al.*, 1991; Sadler *et al.*, 1991).

Various attempts have been made to overcome these problems, including

- The use of pre-classification image transformations and feature-extraction techniques, such as median filters (Atkinson *et al.*, 1985; Sadler *et al.*, 1991) and various measures of image texture (Haralick, 1979; Baraldi and Parmiggiani, 1990; Franklin and Peddle, 1990; Gong and Howarth, 1990; Sadler *et al.*, 1991);
- The incorporation of spatially referenced, ancillary data into the classification procedure (Forster, 1984; Sadler and Barnsley, 1990; Ehlers *et al.*, 1991; Sadler *et al.*, 1991);
- The use of enhanced classification algorithms, ranging from contextual classifiers (Gurney, 1981; Gurney and Townshend, 1983; Gong and Howarth, 1992), through knowledge-based expert systems (Mehldau and Schowengerdt, 1990; Moller-Jensen, 1990), to artificial neural networks (Hepner *et al.*, 1990; Kanellopoulos *et al.*, 1992; Civco, 1993; Dryer, 1993); and
- The application of post-classification spatial processing, ranging from simple majority filters to spatial (or contextual) reclassification procedures (Thomas, 1980; Wharton, 1982a; Wharton, 1982b; Gurney and Townshend, 1983; Gong and Howarth, 1990; Whitehouse, 1990; Guo and Moore, 1991; Gong and Howarth, 1992; Wang and Civco, 1992a; Wang and Civco, 1992b; Eyton, 1993).

However, not all of these techniques directly address the problem of inferring land use from a complex spatial mixture of spectrally distinct land-cover types. For example, pre-classification spatial filtering attempts to circumvent the problem by suppressing some of the spatial variability within the image. This is achieved only at the expense of a reduction in the effective spatial resolution of the data set. It also produces somewhat arbitrary mean vectors for urban land use categories by aggregating the detected spectral responses of their component land-cover types.

Of the other techniques, spatial (or contextual) reclassification represents a comparatively simple way to examine the spatial variation in land cover in remotely sensed images, and is easy to implement in most image processing systems. Spatial reclassification techniques divide the classification process into two stages: the first involves a standard, per-pixel classification of the scene; the second involves some form of post-classification spatial processing of these data. Use of this procedure to infer urban *land use* from the spatial arrangement of land cover was first suggested by Wharton (1982a; 1982b). The assumption underlying this approach is that individual categories of land use have characteristic spatial mixtures of spectrally distinct land cover types that enable their recognition in high spatial resolution images (Wharton, 1982a; Wharton, 1982b; Barnsley and Barr, 1992). For example, residential districts might be characterized by the intermixing of roofs, roads, and gardens.

Spatial reclassification can be performed in one of two ways. The first, referred to as kernel-based spatial reclassification (Gurney and Townshend, 1983; Barnsley and Barr, 1992), involves passing a simple convolution kernel across the land-cover image. In the second, referred to as object-based spatial reclassification (Gurney and Townshend, 1983), discrete "objects" (i.e., groups of adjacent pixels with the same class label) are identified within the initial image segmentation: information on the size, shape, and spatial arrangement of these objects is subsequently used to determine the nature of the land use in different parts of the image (Barr, 1992; Barr and Barnsley, 1993; Barnsley *et al.*, 1993). In this paper, we describe a kernel-based procedure, referred to as SPARK (SPAtial Reclassification Kernel). SPARK examines *both* the frequency *and* the spatial arrangement of class (land-cover) labels within a square kernel. This technique is tested using a subscene extracted from a SPOT-1 HRV multispectral image of south-east London, England.

SPARK: A SPAtial Reclassification Kernel

Background

The work by Wharton (1982a; 1982b) provides an early example of kernel-based spatial re-classification, in which the initial low-level segmentation of the image is performed using a standard, unsupervised classification algorithm. The *frequency* of different land-cover types within each *n*- by *n*-pixel region is then calculated by convolving a simple, rectangular kernel with the classified image. The land use associated with the pixel at the center of the kernel is derived using an unsupervised, non-parametric clustering procedure applied to these frequency data. Similar techniques have been used more recently by Whitehouse (1990), Guo and Moore (1991), Gong and Howarth (1992), and Eyton (1993); although, in these studies, with the exception of Eyton (1993), the frequency distribution of land-cover types surrounding each pixel is compared with those of known areas of the candidate land-use categories.

Although the method developed by Wharton examines the *frequency* with which different class labels occur within the kernel, it does not account for differences in their *spatial arrangement*. The limitation that this imposes is evident in the following example. Consider two separate 3- by 3-pixel windows, each of which has four pixels labeled as the land-cover class "Building." In an industrial or commercial district, where these might represent a single large factory or warehouse, the pixels are likely to be clustered together in a block (Figure 1a). By contrast, in a residential area, where the same class labels might represent individual houses, the "Building" pixels might be arranged in a line (terraced housing) or might be physically separate (detached housing) (Figure 1b). However, a procedure which simply calculates the frequency of different class labels within these windows will have no means of distinguishing these two conditions. The example illustrates the need to find a reliable method for recording both the frequency *and* the spatial arrangement of class labels within a given section of the image. One way to do this is to record the number of times that different class labels occur next to one another within a pre-defined, mov-

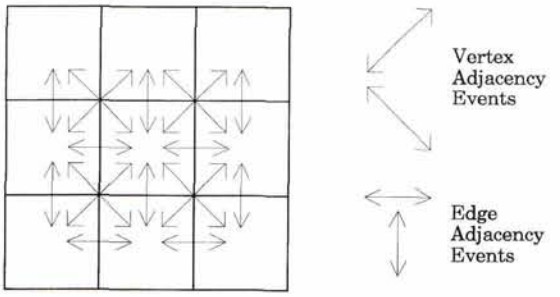

Figure 2. Adjacency events in a 3- by 3-pixel window.

ing window. A simple technique to achieve this, referred to as the SPAtial Reclassification Kernel (SPARK), is described in this paper.

The SPAtial Reclassification Kernel (SPARK)

SPARK operates by examining pairs of adjacent pixels within a square kernel (i.e., those connected along an edge or by a vertex), the size of which is selected by the user (Figure 2). The class label associated with each pixel defines the nature of the "adjacency event." For example, contiguous pixels labeled "Building" and "Tree," respectively, produce a Building-Tree adjacency event. Note that each pair of pixels produces a *single* adjacency event, so that the order of the labels *is not significant: i.e., the adjacency events "Tree-Building"* and "Building-Tree" are identical. Thus, in Figure 1a there are six Building-Building adjacency events, four of Building-Tree, five of Building-Grass, and so on. By comparison, although the window in Figure 1b contains exactly the same number of pixels belonging to each class, there are only three Building-Building adjacency events, but six of Building-Tree.

In practice, SPARK is convolved with the land cover image to produce an adjacency-event matrix, **M**, for each pixel: i.e.,

$$\mathbf{M} \begin{pmatrix} f_{11} & f_{12} & f_{13} & \cdots & f_{1j} \\ & f_{22} & f_{23} & \cdots & f_{2j} \\ & & f_{33} & \cdots & f_{3j} \\ & & & & \vdots \\ & & & & f_{ij} \end{pmatrix} \quad (1)$$

The value of each element, f_{ij}, of the matrix denotes the frequency with which pixels belonging to class i are adjacent to those belonging to class j, for the current position of the kernel. The number of elements in M is determined by the number of classes, C, in the image and is therefore independent of the kernel size. Note that we only consider the upper triangular elements, because $M_{ij} \equiv M_{ji}$. For most studies, where the number of land-cover classes is reasonably small, this represents an efficient means of storing information about the spatial arrangement of the land-cover types within the image. Table 1 shows the adjacency-event matrices for the simulated 3- by 3-pixel windows presented in Figure 1.

The adjacency-event matrix, M, described above, is similar in some respects to the spatial-dependency (or co-occurrence) matrix devised by Haralick (1979), though here we deal with class labels rather than with raw digital numbers (DN). It is also closely related to several of the measures of spatial variability used in landscape ecology, notably "Contagion" (Robinove, 1986; Turner, 1989) and the Binary Comparison Matrix (BCM) developed by Murphy (1985). However, there are several important differences between SPARK and these indices. First, unlike the BCM, the number of elements in SPARK's adjacency-event matrix is independent of the kernel size. Second, SPARK records information on the precise nature of each adjacency event, whereas the BCM simply notes whether adjacent pixels have the same or different class labels. Third, unlike contagion, SPARK examines adjacency between pixels connected vertex-to-vertex, as well as edge-to-edge. Finally, SPARK produces values ranging between 0 and 1, irrespective of the number of classes (*cf.*, contagion).

Assigning Pixels to Land-Use Categories Using SPARK

The land use category, k, for a given pixel is determined by comparing its adjacency-event matrix, M, with those derived from representative sample areas of the candidate land-use categories; the latter will be referred to as "template" matrices, T_k. Note that the sample areas used to generate the template matrices are the same size as the spatial reclassification kernel. Multiple template matrices can be defined for each land use. These may either be used independently or be pooled to produce an "average" template matrix. The advantage of using a series of independent templates for a single land use is that subtle variations in the spatial arrangement of its constituent land-cover types at different locations within the image can be taken into account. However, it also results in a linear increase in computation time. On the other hand, use of pooled or "average" template matrices may result in overlap between land-use classes in "adjacency space."

As the spatial reclassification kernel is passed over the image, the current adjacency-event matrix is compared with each of the template matrices using Equation 2: i.e.,

$$\Delta_k = 1 - \sqrt{0.5N^2 \sum_{i=1}^{C} \sum_{i=j}^{C} (M_{ij} - T_{kij})^2} \quad (2)$$

$$0 \le \Delta_k \le 1 \quad (3)$$

where M_{ij} is an element of the current adjacency-event matrix, T_{kij} is the corresponding element of the template matrix for land-use category k, N is the total number of adjacency events in the kernel (determined by the kernel size, e.g., N = 20 for a 3- by 3-pixel kernel, N= 72 for a 5- by 5-pixel kernel; recall that a pair of adjacent pixels produces a *single* adjacency event), and C is the number of land-cover classes in the image.

The term Δ_k can be thought of as an index of similarity between the current adjacency-event matrix and the template matrix for land-use category k. Thus, a value of 1.0 indicates a perfect match with one of the land-use templates, while a value of 0.0 indicates no match. The pixel at the center of the kernel is, therefore, assigned to the land-use category k for which Δ_k is maximized. A user-specified threshold can be set to prevent pixels being assigned to a land-use category on the basis of a weak match between the measured adjacency-event matrix and a land-use template.

TABLE 1. ADJACENCY-EVENT MATRICES FOR SIMULATED 3- BY 3-PIXEL WINDOWS SHOWN IN FIGURES 1A AND 1B, RESPECTIVELY.

a)	B	G	T
B	6	4	4
G	-	0	4
T	-	-	1

b)	B	G	T
B	3	5	6
G	-	3	2
T	-	-	1

TABLE 2. CONFUSION MATRIX FOR PER-PIXEL LAND-COVER CLASSIFICATION.

LAND COVER TYPE Image ▾ True ▸	Small Structure	Large Structure	Tree	Crop	Grass	Soil	Water
Small Structure	**25**	0	0	0	0	0	0
Large Structure	0	**20**	0	0	0	0	0
Tree	0	0	**156**	0	0	0	0
Crop	0	0	7	**73**	6	0	0
Grass	0	0	0	0	**191**	0	0
Soil	0	3	0	0	0	**91**	0
Water	0	0	0	0	0	0	**18**
Total Test Pixels	25	23	163	73	197	91	18

Average Accuracy	97.09%	Overall Accuracy	97.29%	Kappa Coefficient (x100)	93.0%

Test Area and Satellite Sensor Data

To test SPARK, we selected an area to the southeast of London, England, covering the borough of Bromley. This area encompasses various types of urban land use, ranging from densely occupied early 20th century housing in the northwest, through major shopping areas and inter-war industrial areas in the center, to low-density suburbs in the southeast. Surrounding the urbanized area are very large tracts of open country, many of which are statutorily protected green belt lands.

The image data used in this investigation were extracted from a cloud-free, multispectral (XS) SPOT-1 HRV image of London, England (scene 32, 246; +22.46°) acquired on 30 June 1986 (Figure 3). In particular, a 512- by 512-pixel subsection (covering an area of approximately 10 km by 10 km) of the full image, centered on the town of Orpington, was selected for detailed study. This area exhibits a complex spatial pattern of land cover and land use, providing a stringent test for both conventional and alternative classification techniques. The image data were geometrically corrected to conform to the U.K. national grid and were resampled using nearest-neighbor interpolation prior to further analysis.

Results

Stage 1: Initial Land-Cover Classification.

The first stage in the spatial re-classification procedure is the production of an initial land-cover map from the remotely sensed image. A variety of techniques can be used for this purpose, including unsupervised multispectral classification, region growing, and split-and-merge procedures (Chen and Pavlidis, 1979; Mather, 1987; Li and Muller, 1991). Although most other studies of spatial reclassification have tended to make use of clustering algorithms at this stage, a supervised maximum-likelihood algorithm was employed in this investigation. This is because it is believed to offer the greatest control over both the number and the nature of the classes defined. In this respect, seven broad land-cover classes have been identified in the Orpington subscene: SMALL STRUCTURE, LARGE STRUCTURE, TREE, CROP, GRASS, SOIL, and WATER. The SMALL STRUCTURE class corresponds to roads and buildings within the residential districts of the urban area; no attempt has been made to distinguish between these two surfaces, due to the difficulty in identifying pure pixels of either surface at this spatial resolution. Training areas for a separate class, referred to as LARGE STRUCTURE, have also been identified on the basis of a pronounced contrast between the spectral properties of these areas and those of the SMALL STRUCTURE class. Detailed examination of the digital image (Figure 3) and the corresponding Ordnance Survey 1:10,000-scale base maps suggests that the LARGE STRUCTURE class corresponds to large buildings, such as factories, warehouses, and hospitals, which often have large, flat concrete roofs; these have a much higher reflectance at visible wavelengths than, say, the slate and tile roofs and tarmac roads found in the residential districts. The remaining classes are reasonably self-explanatory. However, it is worth noting that the GRASS class incorporates regions of open space (i.e., gardens and recreational land) within the urban area, as well as fields of permanent pasture lying outside it. Similarly, the CROP class incorporates, and is dominated by, areas of wheat and barley; no attempt has been made to distinguish between these two crops in this particular study.

Irregularly shaped regions, sampled systematically within the image, have been used to define several training areas for each of the candidate land-cover classes. A second set of regions has been used to define an independent test set. Some difficulty was experienced in creating the training and testing sets for the SMALL STRUCTURE, WATER, and LARGE STRUCTURE classes. In the case of WATER and LARGE STRUCTURE, this was because of their relatively limited areal extent, while for the SMALL STRUCTURE class it was primarily due to the comparatively narrow, elongated regions that it forms. Consequently, the number of pixels used to train and to test these classes is quite small (Table 2).

A very low rejection threshold has been set for the maximum-likelihood algorithm (>5 standard deviations, i.e., $<$ 0.001 percent pixels rejected) to produce an image with no unclassified pixels. This is because an adjacency event involving a NULL class pixel (hereafter referred to as a NULL-adjacency event) presents a problem at the reclassification stage. More specifically, a NULL-adjacency event may obscure the true spatial pattern of land-cover types present within the kernel. Thus, a SMALL STRUCTURE-NULL adjacency event may, in reality, represent SMALL STRUCTURE-SMALL STRUCTURE or SMALL STRUCTURE-GRASS, and so on. Moreover, where there is more than one NULL-adjacency event within the kernel, it may be impossible to determine the land use at that location.

The results of the initial classification are presented in Table 2 and Figure 4. Not surprisingly, given the limited

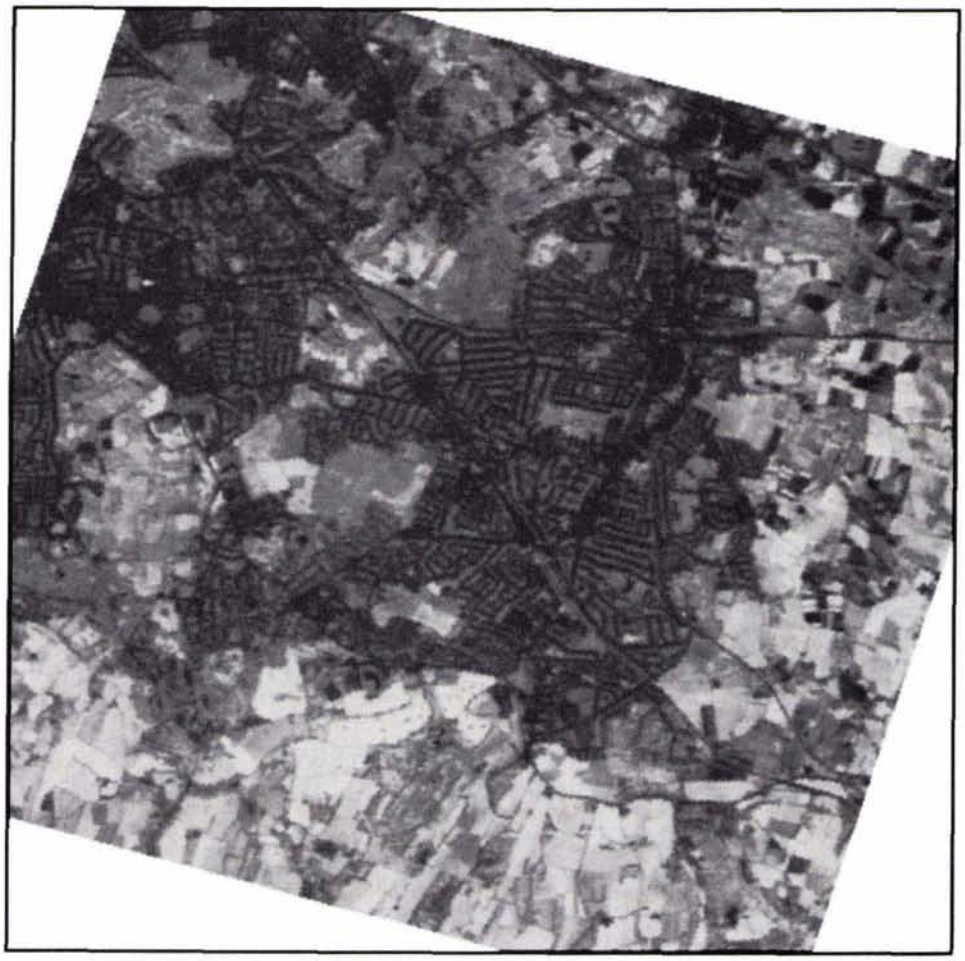

Figure 3. SPOT-1 HRV image of Orpington in the borough of Bromley, southeast London (20-m spatial resolution; near-infrared waveband (XS3)). Note that the road pattern within the urban area is clearly evident.

number and rather broad nature of the land-cover classes identified, a very high level of classification accuracy (overall accuracy = 97.3 percent; Kappa coefficient = 0.93: Congalton *et al.*, 1983; Rosenfield and Fitzpatrick-Lins, 1986) has been achieved; although the use of contiguous blocks of pixels for the test set means that this is probably an overestimate of the true accuracy value.

Stage 2. Spatial Reclassification

Having derived a satisfactory land-cover classification, SPARK has been used to reclassify the image into eight categories of land use: medium-density residential, low-density residential, commercial/industrial, woodland, arable farmland, permanent pasture, vacant/fallow land, and open water. The distinction made here between the medium-density and low-density residential categories is somewhat subjective. However, for the purpose of this study, medium-density housing broadly corresponds to terraced buildings with relatively small gardens, whereas low-density housing corresponds to detached and semi-detached buildings with larger gardens. This division of residential land was made to provide a more stringent test for SPARK.

Given the spatial resolution of the SPOT-HRV images and the range of spatial variation in land cover exhibited by the candidate land-use categories, a 9- by 9-pixel kernel was selected for use in this study. This represents a compromise between the need to account for the full range of spatial variation in land cover exhibited by certain types of land use, such as the two residential categories, and the need to minimize the smoothing effect associated with large kernels.

Template matrices were derived for each land use from 9- by 9-pixel windows sampled at random within larger training areas. To assess the separability of the candidate classes in the training set, Δ_k values (Equation 2) were calculated between each pair of template matrices (Table 3). This is analagous to the use of pairwise-divergence analysis in assessing the spectral separability of candidate classes in a standard multispectral classification. Table 3 demonstrates that the Δ_k values are generally very low ($\Delta_k < 0.37$), indicating that most of the candidate classes exhibit rather different spatial mixtures of land cover. The one clear exception to this is the strong match ($\Delta_k = 0.8$) that exists between the low-density residential and medium-density residential templates. Further analyses, not reported here, indicate that this is also true for other kernel sizes. This suggests that it might prove difficult to distinguish these land-use categories using a simple kernel-based procedure, such as SPARK.

Despite this, a 9- by 9-pixel kernel was applied to the

land-cover image in an attempt to identify all eight land-use categories outlined above (Figure 5). The reclassification accuracy was tested using an independent set of sample areas. The land use in each of these regions was initally determined from recent Ordnance Survey 1:10,000-scale base maps and was subsequently verified through field observation. Table 4 indicates that SPARK performs very well for all of the candidate land-use categories using a 9- by 9-pixel kernel (overall accuracy = 96.86 percent, Kappa coefficient = 0.921: Congalton *et al.*, 1983; Rosenfield and Fitzpatrick-Lins, 1986); even the two residential classes, whose template matrices seemed so similar, appear to be separable in practice.

In addition to examining the standard classification accuracy table (Table 4), it is instructive to analyze the Δ_k values associated with each pixel in Figure 5 (i.e., the strength of the match between the adjacency-event matrix for that pixel and the template matrix for the land-use category to which it was assigned). This is important because we need to be certain that none of the pixels in the image has been assigned to a given land use on the basis of a weak match, because this would reduce our confidence in the resultant land-use map. The results of this analysis are presented in Figures 6 and 7. These indicate that $\Delta_k > 0.5$ (i.e., a good match) for 99 percent of the image, and $\Delta_k > 0.75$ (i.e., a strong match) for approximately 55 percent of the image.

Even where a pixel exhibits a very strong match with one of the template matrices, our confidence in the land use category to which it is assigned may be reduced if that pixel also displays a similarly high Δ_k value for one or more of the other categories. This situation is most likely to arise where the template matrices for the candidate classes are themselves similar, as was shown to be the case in this study for two of the three urban categories (Table 3). To evaluate the significance of this effect, sample areas of these three land uses were identified within the image. The Δ_k values were extracted from each sample area for all three template matrices; summary statistics are presented in Table 5. A difference-of-means test (t-test) was used to examine whether the average Δ_k value for a given sample area was significantly higher for the template matrix of the corresponding land use than for either of the other template matrices. This was, indeed, found to be the case at the 0.01 significance level (i.e., 99 percent confidence level) for all three sample areas.

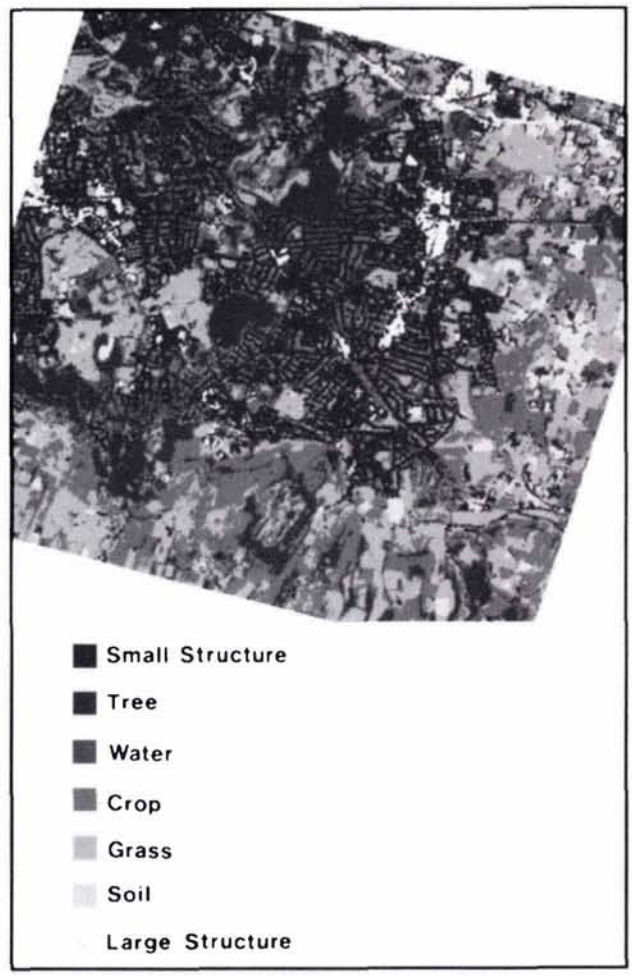

Figure 4. Land-cover classification of the Orpington subscene generated using a standard per-pixel, maximum-likelihood algorithm.

TABLE 3. THE Δ_k VALUES BETWEEN TEMPLATE MATRICES FOR 9- BY 9-PIXEL KERNEL.

Δ_k	Low-Density Residential	Medium-Density Residential	Commercial/ Industrial	Arable Crops	Pasture	Woodland	Bare Soil	Water
Low-Density Residental	1.00	0.80	0.35	0.29	0.37	0.17	0.19	0.17
Medium-Density Residential	-	1.00	0.30	0.18	0.35	0.13	0.14	0.13
Commercial/ Industrial	-	-	1.00	0.20	0.27	0.14	0.18	0.14
Arable Crops	-	-	-	1.00	0.17	0.06	0.07	0.06
Pasture	-	-	-	-	1.00	0.12	0.13	0.12
Woodland	-	-	-	-	-	1.00	0.02	0.02
Bare Soil	-	-	-	-	-	-	1.00	0.00
Water	-	-	-	-	-	-	-	1.00

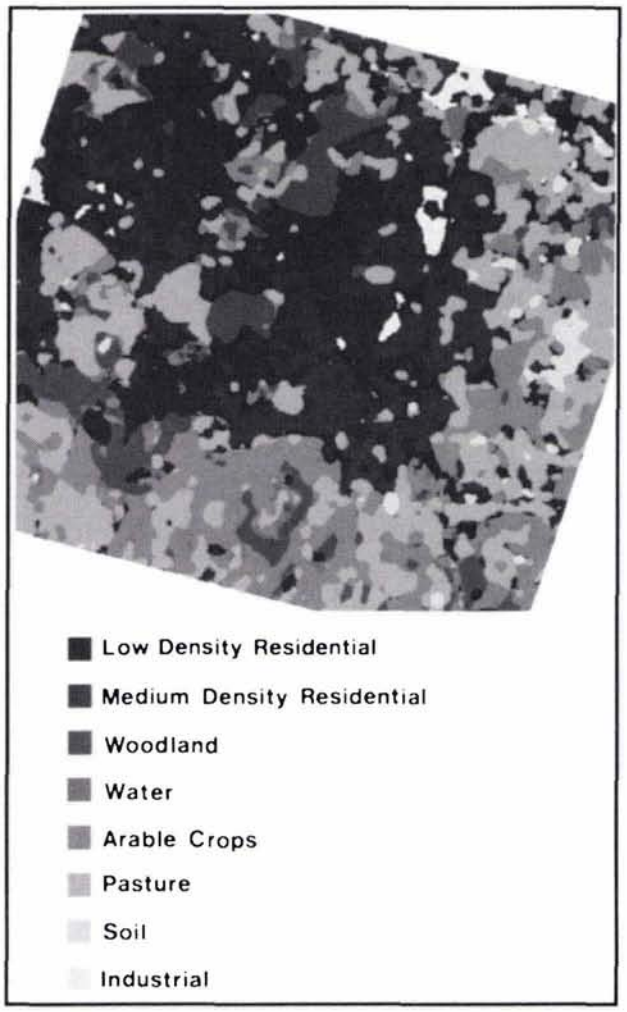

Figure 5. Land-use map produced using the kernel-based spatial reclassification scheme (SPARK) with a 9- by 9-pixel kernel.

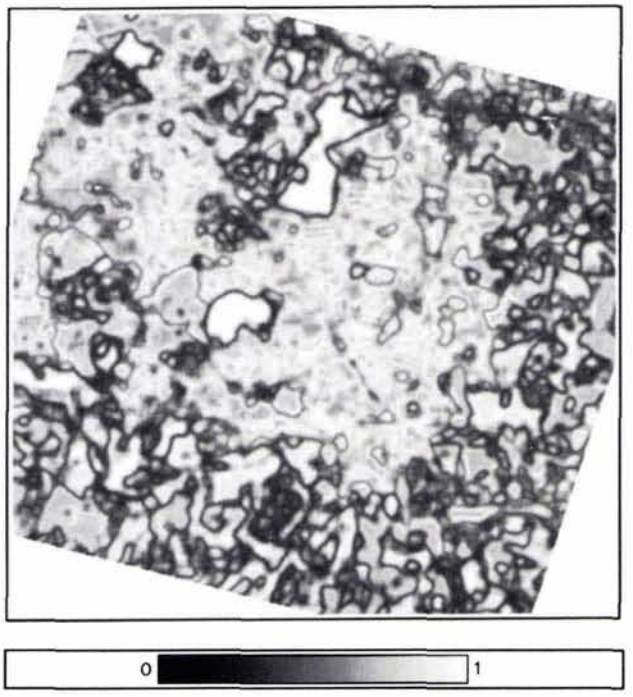

Figure 6. Image showing Δ_k values produced using SPARK with a 9- by 9-pixel kernel applied to the land-cover map of the Orpington sub-scene. High values indicate a good match between the current adjacency-event matrix and one of the land-use templates; low values indicate a weak match.

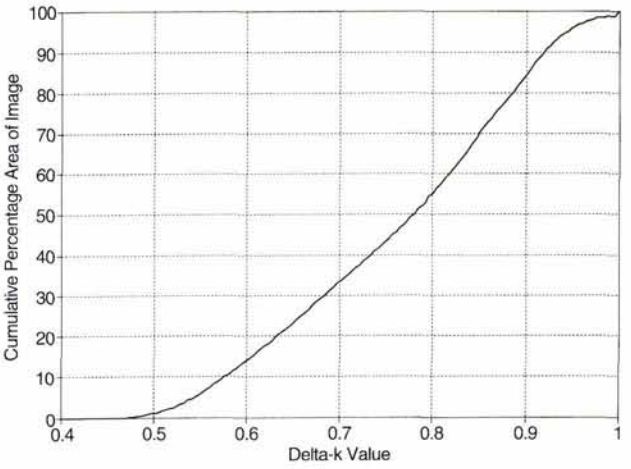

Figure 7. Cumulative area (%) of land-use image versus Δ_k value.

Discussion

This paper has examined the development and application of a kernel-based spatial reclassification procedure (SPARK) designed to infer information on land use from the spatial arrangement of land-cover types within an image. A significant feature of this procedure is that it provides a confidence statistic (Δ_k) for each pixel in the output (land-use) image. Preliminary results obtained using SPARK have proved very encouraging. In particular, it has proved possible to distinguish quite subtle differences in urban land use, notably, two types of residential land that differ principally in terms of housing density, within a subscene extracted from a SPOT-HRV multispectral image of southeast London, England.

Despite this, the basic SPARK algorithm could be improved in two ways: first, by employing different kernel sizes in different parts of the image, and second, by taking account of the "likelihood" (probability) values associated with the class labels in the land-cover image. In terms of the former, it should be noted that, while a small kernel is generally preferable for non-urban areas (to minimize the smoothing effect associated with larger kernels), a large kernel is usually required to represent the full spatial variability of land cover in urban districts. This issue might be addressed through the development of an adaptive SPARK, where the size of the kernel varies according to its position within the image. This, in turn, would require some means of determining the most appropriate kernel size at any given location. Possible options include

- the use of image texture measures, with larger kernels employed over spectrally heterogeneous regions of the image; or

TABLE 4. CONFUSION MATRIX FOR LAND-USE RECLASSIFICATION USING SPARK (9- BY 9-PIXEL KERNEL)

LAND USE True ▸ / Image ▾	Low Density Residential	Medium Density Residential	Commercial / Industrial	Woodland	Arable	Pasture	Fallow/ Vacant	Water
Low Density Residential	**1276**	1	0	0	0	0	0	0
Med. Density Residential	4	**639**	0	0	0	0	0	0
Commercial / Industrial	0	0	**23**	0	0	0	0	0
Woodland	0	0	0	**464**	0	0	1	0
Arable	0	0	0	0	**73**	0	0	0
Pasture	0	0	0	0	0	**197**	0	0
Fallow/Vacant	0	0	0	0	0	0	**81**	0
Water	0	0	0	0	0	0	9	**12**
No. of Test Pixels	1280	640	23	464	73	197	91	12
Size of Training Set	484	224	36	80	72	126	77	15

Average Accuracy	97.98%	Overall Accuracy	96.86%	Kappa Coefficient (%)	92.1%

TABLE 5. THE Δ_A VALUES OBTAINED FOR SAMPLE AREAS OF KNOWN LAND USE AND THREE "URBAN" TEMPLATE MATRICES.

Actual Land Use ▸ / Template Matrix ▾		Low-Density Residential (N=4147)	Medium-Density Residential (N=1708)	Commercial/ Industrial (N=246)
Low-Density Residential	Mean	0.830	0.651	0.436
	St. Dev	0.071	0.059	0.084
Medium-Density Residential	Mean	0.709	0.810	0.328
	St. Dev.	0.091	0.071	0.098
Commerical / Industrial	Mean	0.364	0.293	0.880
	St. Dev.	0.042	0.062	0.072

- the use of ancillary data (e.g., previous land-use classifications of the study area) to divide the image into discrete segments for separate processing using different kernel sizes.

The second potential improvement would be to take account of the "likelihood" (probability) that each pixel in the land-cover image belongs to the cover type indicated by its class label. This information might be obtained directly from the maximum-likelihood algorithm used to generate the land-cover image. The product of the "likelihood" values for adjacent pixels might then be used to establish a probability value for that particular adjacency event. For example, contiguous pixels labeled "Built" and "Tree" with, respectively, likelihood values of 0.8 and 0.7 would produce a Built-Tree adjacency event with a probability value of 0.56. This information might, in turn, be used to modify the measured adjacency-event matrix.

In pursuing this point, it is worth noting that any technique which attempts to infer land use by examining the spatial pattern of land cover in an image will be sensitive to the accuracy of the initial land-cover classification. The degree of sensitivity has not been assessed in this paper, but will be the subject of future study. This might be achieved by providing SPARK with several land-cover images of the same scene, produced using slightly different training sets or, possibly, different classification algorithms. It will also be important to examine SPARK's dependence on both the *number* and *nature* of the candidate land-cover classes used at this stage.

Finally, although SPARK has proved successful with 20-m-resolution data, the range of spatial scales over which it is applicable has yet to be determined. This will be controlled by the interaction between the spatial resolution of the sensor and the spatial variation in land cover in the corresponding scene. At one extreme, SPARK will cease to be applicable where the spectral response of several scene elements is averaged over the IFOV of the sensor, to produce a homogeneous, composite signal. For most urban areas in the United Kingdom, this limit is approached in image data acquired by sensors such as the Landsat Multispectral Scanning System (MSS). The other limit of applicability is more difficult to define.

Conclusions

A number of conclusions can be drawn from this study. First, it appears possible to derive information on urban land use from an analysis of both the *frequency* and the *spatial arrangement* of class labels in land-cover data produced from multispectral images acquired by a high spatial resolution satellite sensors. Second, kernel-based spatial reclassification procedures represent a relatively simple method by which this can be achieved. The development and application of one such technique, known as SPARK (SPAtial Reclassification Kernel), has been described in this paper. SPARK is able to distinguish quite subtle differences in land use within and around urban areas. It is also easy to implement in most image processing systems, running on PC platforms upwards. Finally, a number of potential improvements to the basic SPARK algorithm have been suggested; it is believed that, when implemented, these will increase both the accuracy and the sensitivity of this technique.

Acknowledgments

The authors would like to thank the U.K.'s Economic and Social Research Council and Natural Environment Research Council (NERC) for support through a research grant under their joint program on Geographical Data Handling. We would also like to acknowledge the help and advice of various colleagues, especially Kevin Morris (NERC Image Analysis Unit, University of Plymouth, U.K.), Graham Sadler (Arthur Anderson Consulting), and Andrew Williams (Kingston College, U.K.). Thanks are also due to Prof. Paul Mather (University of Nottingham, U.K.) for providing support and advice in his rôle as coordinator of the ESRC/NERC Geographical Data Handling program. Finally, the authors would like to thank the anonymous referees for their helpful comments and constructive criticism.

References

Atkinson, P., J.L. Cushnie, J.R.G. Townshend, and A.K. Wilson, 1985. Improving Thematic Mapper land cover classification using filtered data, *International Journal of Remote Sensing,* 6:955–961.

Baraldi, A., and F. Parmiggiani, 1990. Urban area classification by multispectral SPOT images, *IEEE Transactions on Geoscience and Remote Sensing,* 28:674–680.

Barnsley, M.J., S.L. Barr, A. Hamid, J–P. Muller, G.J. Sadler, and J.W. Shepherd, 1993. Analytical tools to monitor urban areas, *Geographical Information Handling – Research and Applications* (P. Mather, editor), John Wiley, Chichester, pp. 147–184.

Barnsley, M.J., and S.L. Barr, 1992. Developing kernel-based spatial re-classification techniques for improved land-use monitoring using high spatial resolution images, *Proc. XXIX Conference of the International Society for Photogrammetry and Remote Sensing (ISPRS'92), International Archives of Photogrammetry and Remote Sensing : Commission 7,* Washington D.C., 2–14 August 1992, pp. 646–654.

Barnsley, M.J., S.L. Barr, and G.J. Sadler, 1991. Spatial re-classification of remotely sensed images for urban land use monitoring, *Proceedings of Spatial Data 2000,* Oxford, 17–20 September, Remote Sensing Society, Nottingham, pp. 106–117.

Barnsley, M.J., G.J. Sadler, and J.S. Shepherd, 1989. Integrating remotely–sensed images and digital map data in the context of urban planning, *Proceedings of the 15th Annual Conference of the Remote Sensing Society,* Bristol, U.K., 13–15 September, Remote Sensing Society, Nottingham, pp. 25–32.

Barr, S.L., 1992. Object–based re–classification of high resolution digital imagery for urban land use monitoring, *Proc. XXIX Conference of the International Society for Photogrammetry and Remote Sensing (ISPRS'92), International Archives of Photogrammetry and Remote Sensing : Commission 7,* Washington D.C., 2–14 August, pp. 969–976.

Barr, S.L., and M.J. Barnsley, 1993. Object-based spatial analytical tools for urban land-use monitoring in a raster processing environment, *Proceedings of the Fourth European Conference on Geographical Information Systems (EGIS'93),* Genoa, Italy, April, pp. 810–822.

Chen, P.C., and T. Pavlidis, 1979. Segmentation by texture using a co-occurrence matrix and a split-and-merge algorithm, *Computer Vision, Graphics and Image Processing,* 10:172–182.

Civco, D.C., 1993. Artificial neural networks for land-cover classification and mapping, *International Journal of Geographical Information Systems,* 7:173–186.

Congalton, R.G., R.G. Oderwald, and R.A. Mead, 1983. Assessing Landsat classification accuracy using discrete multivariate statistical techniques, *Photogrammetric Engineering & Remote Sensing,* 49:1671–1678.

Dryer, P., 1993. Classification of land cover using optimized neural nets on SPOT data, *Photogrammetric Engineering & Remote Sensing,* 59:617–621.

Ehlers, M., D. Greenlee, T. Smith, and Star, 1991. Integration of remote sensing and GIS: Data and data access, *Photogrammetric Engineering & Remote Sensing,* 57:669–675.

Eyton, J.R., 1993. Urban land use classification and modelling using cover-type frequencies, *Applied Geography,* 13:111–121.

Forster, B.C., 1980. Urban residential ground cover using Landsat digital data, *Photogrammetric Engineering & Remote Sensing,* 46:547–558.

———, 1984. Combining ancillary and spectral data for urban applications, *International Archives of Photogrammetry and Remote Sensing,* pp. 55–67.

———, 1985. An examination of some problems and solutions in monitoring urban areas from satellite platforms, *International Journal of Remote Sensing,* 6:139–151.

Franklin, S.E., and D.R. Peddle, 1990. Classification of SPOT-HRV imagery and texture features, *International Journal of Remote Sensing,* 11:551–556.

Gastellu-Etchegorry, J.P., 1990. An assessment of SPOT XS and Landsat MSS data for digital classification of near–urban land cover, *International Journal of Remote Sensing,* 11:225–235.

Gong, P., and P.J. Howarth, 1990. The use of structural information for improving land-cover classification accuracies at the rural–urban fringe, *Photogrammetric Engineering & Remote Sensing,* 56:67–73.

———, 1992. Frequency-based contextual classification and gray-level vector reduction for land-use identification, *Photogrammetric Engineering & Remote Sensing,* 58:423–437.

Guo, Liu Jian, and J. McM. Moore, 1991. Post–classification processing for thematic mapping based on remotely-sensed image data: *Proceedings of the International Conference of IEEE Geoscience and Remote Sensing Society,* Espoo, Finland, 3–7 June, IEEE, New York, pp. 2203–2206.

Gurney, C.M., 1981. The use of contextual information to improve land cover classification of digital remotely sensed data, *International Journal of Remote Sensing,* 2:379–388.

Gurney, C.M., and J.R.G. Townshend, 1983. The use of contextual information in the classification of remotely sensed data, *Photogrammetric Engineering & Remote Sensing,* 49:55–64.

Haack, B., N. Bryant, and S. Adams, 1987. An assessment of Landsat MSS and TM data for urban and near-urban land-cover digital classification, *Remote Sensing of Environment,* 21:201–213.

Haralick, R.M., 1979. Statistical and structural approaches to texture, *Proceedings of the IEEE,* 67:786–804.

Hepner, G.F., T. Logan, N. Ritter, and N. Bryant, 1990. Artificial neural network classification using a minimal training set: Comparison to conventional supervised classification, *Photogrammetric Engineering & Remote Sensing,* 56:469–473.

Jackson, M.J., P. Carter, T.F. Smith, and W. Gardner, 1980. Urban land mapping from remotely sensed data, *Photogrammetric Engineering & Remote Sensing,* 46:1041–1050.

Kanellopoulos, I., A. Varfis, G.G. Wilkinson, and J. Megier, 1992. Land-cover discrimination in SPOT HRV imagery using an artificial neural network – A 20-class experiment, *International Journal of Remote Sensing,* 13:917–924.

Li, K., and J–P. Muller, 1991. Segmenting satellite imagery: A region growing scheme, *Proceedings of the Conference of the IEEE Geoscience and Remote Sensing Society (IGARSS'91),* Vol. 2, Espoo, Finland, pp. 1075–1078.

Martin, L.R.G., P.J. Howarth, and G. Holder, 1988. Multispectral classification of land use at the rural-urban fringe using SPOT data, *Canadian Journal of Remote Sensing,* 14:72–79.

Mather, P.M., 1987. *Computer Processing of Remotely-Sensed Images,* John Wiley, London, pp. 289–309.

Mehldau, G., and R.A. Schowengerdt, 1990. A C-extension for rule–based image classification systems, *Photogrammetric Engineering & Remote Sensing,* 56:887–892.

Moeller-Jensen, L., 1990. Knowledge-based classification of an urban area using texture and context information in a Landsat-TM image, *Photogrammetric Engineering & Remote Sensing, 56:899–904.*

Murphy, D.L., 1985, Estimating neighborhood variability with a binary comparison matrix, Photogrammetric Engineering & Remote Sensing, 51:667–674.

Robinove, C.J., 1986. Spatial diversity index mapping of classes in

grid cell maps, *Photogrammetric Engineering & Remote Sensing*, 52:1171–1173.

Rosenfield, G.H., and K. Fitzpatrick-Lins, 1986. A coefficient of agreement as a measure of thematic classification accuracy, *Photogrammetric Engineering & Remote Sensing*, 52:223–227.

Sadler, G.J., and M.J. Barnsley, 1990. Use of population density data to improve classification accuracies in remotely-sensed images of urban areas, *Proceedings of the First European Conference on Geographical Information Systems (EGIS'90)*, Amsterdam, The Netherlands, 10–13 April, EGIS Foundation, Utrecht, pp. 968–977.

Sadler, G.J., M.J. Barnsley, and S.L. Barr, 1991. Information extraction from remotely-sensed images for urban land analysis, *Proceedings of the Second European Conference on Geographical Information Systems (EGIS'91)*, Brussels, Belgium, April, EGIS Foundation, Utrecht, pp. 955–964.

Thomas, I.L., 1980. Spatial post-processing of spectrally classified Landsat data, *Photogrammetric Engineering & Remote Sensing*, 46:1201–1206.

Toll, D.L., 1985. Effect of Landsat Thematic Mapper sensor parameters on land cover classification, *Remote Sensing of Environment*, 17:129–140.

Turner, M.G., 1989. Landscape ecology: The effect of pattern on process, *Annual Review Ecological Systems*, 20:171–197.

Wang, Y., and D. Civco, 1992. Spatial modeling-based post-classification of satellite remote sensing data for improved land cover mapping, *Proc. ASPRS/ACSM/RT'92 Convention*, Washington, D.C., 4:122–132.

———, 1992. Post-classification of misclassified pixels by evidential reasoning: A GIS approach for improving classification accuracy of remote sensing data, *Proc. ASPRS/ACSM/RT'92 Convention*, Washington, D.C., 4:160–170.

Wharton, S.W., 1982a. A contextual classification method for recognizing land use patterns in high resolution remotely–sensed data, *Pattern Recognition*, 15:317–324.

———, 1982b. A context-based land use classification algorithm for high resolution remotely sensed data, *Journal of Applied Photographic Engineering*, 8:46–50.

Whitehouse, S., 1990. A spatial land-use classification of an urban environment using high-resolution multispectral satellite data, *Proceedings of the 16th Annual Conference of the Remote Sensing Society, Remote Sensing and Global Change*, Swansea, U.K., 19–21 September, Remote Sensing Society, Nottingham, pp. 433–437.

Woodcock, C.E., and A.H. Strahler, 1987. The factor of scale in remote sensing, *Remote Sensing of Environment*, 21:311–332.

(Received 28 September 1993; revised and accepted 7 October 1994; revised 18 January 1995)

Forthcoming Articles

Articles listed in the August Forthcoming Articles are those scheduled to run through February 1997.

Michael Abrams, Remo Bianchi, and *Dave Pieri,* Revised Mapping of Lava Flows on Mount Etna, Sicily.

M. Aniya, H. Sato, R. Naruse, P. Skvarca, and *G. Casassa,* The Use of Satellite and Airborne Imagery to Inventory Outlet Glaciers of the Southern Patagonia Icefield, South America.

Ling Bian and *Eric West,* GIS Modeling of Elk Calving Habitat in a Priairie Environment with Statistics.

M. Les Bober, Duncan Wood, and *Raymond A. McBride,* Use of Digital Image Analysis and GIS to Assess Regional Soil Compaction Risk.

Timothy L. Bowers and *Lawrence C. Rowan,* Remote Mineralogic and Lithologic Mapping of the Ice River Alkaline Complex, British Columbia, Canada, Using AVIRIS Data.

Pat S. Chavez, Jr., Image-Based Atmospheric Corrections—Revised and Improved.

O. Dikshit and *D.P. Roy,* An Empirical Investigation of Image Resampling Effects upon the Spectral and Textural Supervised Classification of a High Spatial Resolution Multispectral Image.

Leila M.G. Fonseca and *B.S. Manjunath,* Registration Techniques for Multisensor Remotely Sensed Imagery.

Bruno Garguet-Duport, Jacky Girel, Jean-Marc Chassery, and *Guy Pautou,* The Use of Multiresolution Analysis and Wavelets Transform for Merging SPOT Panchromatic and Multispectral Image Data.

Greg G. Gaston, Peggy M. Bradley, Ted S. Vinson, and *Tatayana P. Kolchugina,* Forest Ecosystem Modeling in the Russian Far East Using Vegetation and Land-Cover Regions Identified by Classification of GVI.

Philip T. Giles and *Steven E. Franklin,* Comparison of Derivative Topographic Surfaces of a DEM Generated from Stereoscopic SPOT Images with Field Measurements.

Clyde C. Goad and *Ming Yang,* A New Approach to Precision Airborne GPS Positioning for Photogrammetry.

Joachim Höhle, Experience with the Production of Digital Orthophotos.

Collin G. Homer, R. Douglas Ramsey, Thomas C. Edwards, Jr., and *Allan Falconer,* Landscape Cover-Type Mapping Modeling Using a Multi-Scene Thematic Mapper Mosaic.

Pamela E. Jansma and *Harold R. Lang,* Applications of Spectral Stratigraphy to Upper Cretaceous and Tertiary Rocks in Southern Mexico: Tertiary Graben Control on Volcanism.

N.G. Kardoulas, A.C. Bird, and *A.I. Lawan,* Geometric Correction of SPOT and Landsat Imagery: A Comparison of Map and GPS Derived Control Points.

Steven T. Knick, John T. Rotenberry, and *Thomas J. Zarriello,* Supervised Classification of Landsat Thematic Mapper Imagery in a Semi-Arid Rangeland by Nonparametric Discriminant Analysis.

Jacek Komorowski-Blaszczynski, Landform Characterization with Geographic Information Systems.

Amnon Krupnik, Using Theoretical Intensity Values as Unknowns in Multiple-Patch Least-Squares Matching.

Kenneth C. McGwire, Cross-Validated Assessment of Geometric Accuracy.

Sunil Narumalani, John R. Jensen, Shan Burkhalter, John D. Althausen, and *Halkard E. Mackey, Jr.,* Aquatic Macrophyte Modeling Using GIS and Logistic Multiple Regression.

Paul Pope, Ed Van Eeckhout, and *Cheryl Rofer,* Waste Site Characterization through Digital Analysis of Historical Aerial Photographs.

Tian-Yuan Shih, The Sign Permutation in the Rotation Matrix and the Formulation of Collinearity and Coplanarity Equations.

C.R. de Souza Filho, S.A. Drury, A.M. Denniss, R.W.T. Carlyon, and *D.A. Rothery,* Restoration of Corrupted Optical Fuyo-1 (JERS-1) Data Using Frequency Domain Techniques.

R.D. Spencer, M.A. Green, and *P.H. Biggs,* Integrating Eucalypt Forest Inventory and GIS in Western Australia.

M.D. Tomer, J.L. Anderson, and *J.A. Lamb,* Assessing Corn Yield and Nitrogen Uptake Variability with Digitized Aerial Infrared Photographs.

A.P. van Deventer, A.D. Ward, P.H. Gowda, and *J.G. Lyon,* Using Thematic Mapper Data to Identify Contrasting Soil Plains and Tillage Practices.

Jim Vrabel, Multispectral Imagery Band Sharpening Study.

Jianjun Wang, Gary J. Robinson, and *Kevin White,* A Fast Solution to Local Viewshed Computation Using Grid-Based Digital Elevation Models.

Eric A. Williams and *Dennis E. Jelinski,* On Using the NOAA AVHRR "Experimental Calibrated Biweekly Global Vegetation Index."

Zhangshi Yin and *T.H. Lee Williams,* Obtaining Spatial and Temporal Vegetation Data from Landsat MSS and AVHRR/NOAA Satellite Images for a Hydrologic Model.

David A. Yocky, Multiresolution Wavelet Decomposition Image Merger of Landsat Thematic Mapper and SPOT Panchromatic Data.